Molecular Pharmacology Fast Forward. Published on February 20, 2015 as DOI: 10.1124/mol.114.097550
This article has not been copyedited and formatted. The final version may differ from this version.



**TITLE PAGE**

# Synthetic metallochaperone ZMC1 rescues mutant p53 conformation by transporting zinc into cells as an ionophore

Adam R. Blanden, Xin Yu, Aaron J. Wolfe, John A. Gilleran, David J. Augeri, Ryan S. O'Dell, Eric C. Olson, S. David Kimball, Thomas J. Emge, Liviu Movileanu, Darren R. Carpizo, and Stewart N. Loh

Primary Laboratory of Origin: Loh Lab, Upstate Medical University

Department of Biochemistry and Molecular Biology, SUNY Upstate Medical University, Syracuse, NY 13210 (ARB, SNL)

Rutgers Cancer Institute of New Jersey, New Brunswick, NJ 08903 (XY, DRC)

Department of Surgery, Rutgers Robert Wood Johnson Medical School, New Brunswick, NJ 08903 (XY, DRC)

Department of Physics, Syracuse University, Syracuse, NY 13244 (AJW, LM)

Office of Translational Sciences, Rutgers University, New Brunswick, NJ 08901 (JAG, DJA, SDK)

Department of Neuroscience and Physiology, SUNY Upstate Medical University, Syracuse, NY 13210 (RSO, ECO)

Department of Chemistry and Chemical Biology, Rutgers University, New Brunswick, NJ 08903 (TJE)

Downloaded from molpharm.aspetjournals.org at ASPET Journals on April 17, 2024

Molecular Pharmacology Fast Forward. Published on February 20, 2015 as DOI: 10.1124/mol.114.097550
This article has not been copyedited and formatted. The final version may differ from this version.



**RUNNING TITLE PAGE**

a) Running Title: ZMC1 reactivates mutant p53 by transporting $Zn^{2+}$

b) Correspondence should be addressed Stewart N. Loh
email: lohs@upstate.edu.
phone: (315) 464-8731
fax: (315) 464-8750
address: 4249 Weiskotten Hall, 766 Irving Avenue, Syracuse, NY, 13210.

c) Double spaced text pages (Sections 1-9): 19

Number of Tables: 1

Number of Figures: 5

Number of References: 30

Words in Abstract: 217

Words in Introduction: 928

Words in Discussion: 820

d) Abbreviations: apoDBD - $Zn^{2+}$-free p53 DNA-Binding Domain, DBD - p53 DNA-Binding Domain, DLS - Dynamic Light Scattering, DMEM - Dulbecco's Modified Eagle Medium, DOPC - 1,2-dioleoyl-sn-glycero-3-phosphocholine, EBSS - Earle's Balanced Salt Solution, FBS - Fetal Bovine Serum, FZ3-AM - FluoZin-3-Acetoxymethyl Ester, MC - Metallochaperone, NTA - Nitrilotriacetic Acid, PYR - Pyrithione, ROI - Region of Interest, RZ-3, RhodZin-3, TPEN - N,N,N',N'-tetrakis(2-pyridylmethyl)ethane-1,2-diamine, WT - Wild-Type, ZMC1 - Zinc Metallochaperone-1

Downloaded from molpharm.aspetjournals.org at ASPET Journals on April 17, 2024

Molecular Pharmacology Fast Forward. Published on February 20, 2015 as DOI: 10.1124/mol.114.097550
This article has not been copyedited and formatted. The final version may differ from this version.



## ABSTRACT

p53 is a $Zn^{2+}$-dependent tumor suppressor inactivated in >50% of human cancers. The most common mutation, R175H, inactivates p53 by reducing its affinity for the essential zinc ion, leaving the mutant protein unable to bind the metal in the low $[Zn^{2+}]_{free}$ environment of the cell. The exploratory cancer drug ZMC1 was previously demonstrated to reactivate this and other $Zn^{2+}$-binding mutants by binding $Zn^{2+}$ and buffering it to a level such that $Zn^{2+}$ can repopulate the defective binding site, but how it accomplishes this in the context of living cells and organisms is unclear. Here, we demonstrate that ZMC1 increases intracellular $[Zn^{2+}]_{free}$ by functioning as a $Zn^{2+}$ ionophore, binding $Zn^{2+}$ in the extracellular environment, diffusing across the plasma membrane, and releasing it intracellularly. It raises intracellular $[Zn^{2+}]_{free}$ in cancer (TOV112D) and non-cancer (HEK293) cell lines to 15.8 and 18.1 nM, respectively, with half times of 2-3 min. These $[Zn^{2+}]_{free}$ are predicted to result in ~90% saturation of p53-R175H, thus accounting for its observed reactivation. This mechanism is supported by the x-ray crystal structure of the $[Zn(ZMC1)_2]$ complex, which demonstrates structural and chemical features consistent with those of known metal ionophores. These findings provide a physical mechanism linking ZMC1's *in vitro* and *in vivo* activities, and define the remaining critical parameter necessary for developing synthetic metallochaperones for clinical use.

Downloaded from molpharm.aspetjournals.org at ASPET Journals on April 17, 2024

Molecular Pharmacology Fast Forward. Published on February 20, 2015 as DOI: 10.1124/mol.114.097550
This article has not been copyedited and formatted. The final version may differ from this version.



**INTRODUCTION**

Since its discovery in 1979, the tumor suppressor p53 has become one of the most universally recognized and well-studied proteins in cancer biology (Levine and Oren, 2009). As many as 50% of human cancers harbor mutations in p53, and the last three decades of research have firmly established that loss of p53 function is a key event in the development of many cancers (Olivier *et al.*, 2010). Despite the prevalence of p53 mutations in cancer and clear indications that restoration of p53 function can be therapeutic, developing drugs with this activity has proven a challenge as evidenced by the lack of clinically available therapies that target mutant p53 (Ventura *et al.*, 2007, p. 53; Xue *et al.*, 2007).

One of the most common ways that p53 becomes inactivated is by mutational disruption of a critical $Zn^{2+}$-binding interaction in its DNA-binding domain (DBD) (Olivier *et al.*, 2010). Each p53 monomer coordinates a single $Zn^{2+}$ via C176, C238, C242, and H179 (Cho *et al.*, 1994). Biophysical studies have shown that removal of $Zn^{2+}$ from wild-type (WT) DBD reduces the folding free energy by 30%, alters the conformation of the DNA-binding surface, and reduces sequence-specific DNA binding affinity by 10-fold, to the point where DBD can no longer discriminate between consensus and non-consensus DNA sequences (Butler and Loh, 2003). Cellular studies have also demonstrated that zinc chelation functionally inactivates p53-WT, inhibiting its transcriptional activity and causing it to adopt a mutant-like immunological phenotype (Méplan *et al.*, 2000).

The most common p53 mutation in cancer, R175H, was originally classified as one such $Zn^{2+}$ binding mutant by Fersht et. al. based on its decreased folding energy, diminished DNA-binding affinity, and proximity to the $Zn^{2+}$ binding site (Bullock *et al.*, 1997, 2000). Later studies demonstrated that DBD-R175H exhibits markedly reduced $Zn^{2+}$ binding affinity relative to WT

Downloaded from molpharm.aspetjournals.org at ASPET Journals on April 17, 2024

Molecular Pharmacology Fast Forward. Published on February 20, 2015 as DOI: 10.1124/mol.114.097550
This article has not been copyedited and formatted. The final version may differ from this version.



(Butler and Loh, 2003). We recently measured the dissociation constant of the native DBD-R175H/$Zn^{2+}$ interaction ($K_{d1}$ = 2.1 nM), and found it to be 10-1000-fold higher than the typical intracellular $[Zn^{2+}]_{free}$ of $10^{-12}$-$10^{-10}$ M (Colvin *et al.*, 2010; Yu *et al.*, 2014). We therefore concluded that p53-R175H is non-functional in the cell because it is unable to bind $Zn^{2+}$ under physiologic conditions. We also measured the dissociation constant for $Zn^{2+}$ binding to one or more non-native sites ($K_{d2} \geq 1$ μM) that are likely formed by non-native combinations of the 10 Cys and 9 His residues in DBD. $Zn^{2+}$ binding to these improper ligands causes DBD to misfold and aggregate (Butler and Loh, 2007). In that same study we investigated the mechanism of p53-R175H reactivating compound ZMC1 (Fig. 1A). We found that ZMC1 is a $Zn^{2+}$ buffer *in vitro* and we proposed that it functions as a synthetic metallochaperone (MC) *in vivo* (Yu *et al.*, 2014).

By our definition a synthetic MC must possess two activities. It must increase the free concentration of metal ion inside the cell, and then it must buffer that concentration to the range appropriate to metallate the client protein. Importantly, a synthetic MC need not bind its client, but can function solely through manipulation of free metal. Because ZMC1 binds $Zn^{2+}$ with a dissociation constant ($K_{d,ZMC1}$ = 30 nM) between $K_{d1}$ and $K_{d2}$, it buffers $[Zn^{2+}]_{free}$ to a level high enough to occupy the native zinc binding site, thus restoring WT structure and function to purified DBD-R175H *in vitro* and p53-R175H in cells, but not so high as to populate the non-native sites and induce misfolding. This fulfills one criterion. However, evidence of the ZMC1-mediated increase in intracellular $[Zn^{2+}]$ required by our model has thus far been absent, and if it does occur the source of metal and the mechanism of its increase are unknown.

Negative control compounds A6 and NTA (Fig. 1A) provide some clues regarding the mechanism of ZMC1 (10). A6 is nearly identical in structure to ZMC1 but it binds $Zn^{2+}$ 100-fold less tightly ($K_{d,A6}$ = 1.1 μM). A6 fails to rescue either purified DBD-R175H *in vitro* or p53-

Downloaded from molpharm.aspetjournals.org at ASPET Journals on April 17, 2024

Molecular Pharmacology Fast Forward. Published on February 20, 2015 as DOI: 10.1124/mol.114.097550
This article has not been copyedited and formatted. The final version may differ from this version.



R175H in cells. By contrast, NTA binds $Zn^{2+}$ with affinity similar to that of ZMC1 ($K_{d,NTA}$ = 17 nM), but is polar and negatively charged. NTA restores WT structure to DBD-R175H *in vitro*, but fails to activate p53-R175H in cells except at very high (millimolar) concentrations. The ineffectiveness of A6 and the discrepancy between the *in vitro* and cellular activities of NTA suggests that membrane permeability of the $Zn^{2+}$-bound complex might be important for MC activity.

Here we test the hypothesis that the second defining characteristic of a synthetic MC, besides having the appropriate affinity for the metal, is its ionophore potential, i.e. its ability to transport metal ions into cells (Loh, 2010). In this study we demonstrate that micromolar concentrations of ZMC1, but not NTA or A6, increase intracellular $[Zn^{2+}]_{free}$ and that this increase occurs in both cancer and non-cancer cells. We show that the source of $Zn^{2+}$ is extracellular, and that ZMC1 transports the metal across the plasma membrane as a transition metal specific ionophore. We substantiate this mechanism by solving the $[Zn(ZMC1)_2]$ complex crystal structure, which demonstrates structural and chemical similarity to known metal ionophores. We quantify the resultant intracellular $[Zn^{2+}]_{free}$ and find that it is in the range predicted to maximally reactivate p53-R175H, that this increase happens in minutes, and that it occurs both in the cytosol and nucleus. We also demonstrate that depletion of extracellular $Zn^{2+}$ abrogates ZMC1 function. These results provide the first evidence of a $Zn^{2+}$-ionophore as a p53 reactivating compound, validate the MC model of ZMC1 function, and provide critical information that will facilitate the development of $Zn^{2+}$-MCs as mutant p53 targeted anti-cancer drugs.

Downloaded from molpharm.aspetjournals.org at ASPET Journals on April 17, 2024

Molecular Pharmacology Fast Forward. Published on February 20, 2015 as DOI: 10.1124/mol.114.097550
This article has not been copyedited and formatted. The final version may differ from this version.



## MATERIALS AND METHODS

### Reagents

FZ3-AM, and RZ-3 ($K^+$ salt), and cell culture media were purchased from Life Technologies. DOPC was purchased from Avanti Polar Lipids. ZMC1 and A6 were obtained as previously described (Yu *et al.*, 2014). $[Zn(ZMC1)_2]$ was synthesized and crystallized as detailed in (Supplemental Methods). HEK293 and TOV112D cells were purchased from ATCC and maintained in DMEM + GlutaMAX with 10% FBS and 1 mg/mL penicillin-streptomycin under a 5% $CO_2$ atmosphere at 37 ˚C. All non-cell based experiments were conducted in 50 mM Tris pH 7.2, 0.1 M NaCl at 25 ˚C.

### Liposome Import Assay

DOPC-liposomes were prepared by film rehydration and extrusion as detailed in (Supplemental Methods). The size distribution was determined by dynamic light scattering (DLS) using a Malvern Zetasizer Nano ZS (Supplemental Figure 1). Fluorescence measurements were taken on a Horiba Fluoromax-4 spectrofluorimeter in a 5 x 5 mm quartz cuvette with $\lambda_{ex}/\lambda_{em}$ = 550/572 nm for RZ-3 and 490/515 nm for calcein. Initial $Zn^{2+}$ import/export was quantified by fitting the first 10-30 s of data after each treatment to a line and converted to units of flux using Eqn 1:

Eqn 1:

$$J_i = \frac{\Delta F}{\Delta t} \cdot \left( \frac{F_{max} - F_{min}}{[RZ3]} \right) \cdot \left( \frac{SA}{Vol} \right)$$

where $J_i$ is the initial flux, $\Delta F/\Delta t$ is the slope of the fit line, $F_{max}$ is RZ-3 fluorescence in the presence of saturating $Zn^{2+}$ and 1% TritonX-100, $F_{min}$ is RZ-3 fluorescence in the presence of excess EDTA and 1% TritonX-100, [RZ3] is the concentration of encapsulated RZ-3, and SA/Vol is the surface area to volume ratio calculated assuming hollow spheres of the mean diameter determined by DLS.



Downloaded from molpharm.aspetjournals.org at ASPET Journals on April 17, 2024

Molecular Pharmacology Fast Forward. Published on February 20, 2015 as DOI: 10.1124/mol.114.097550
This article has not been copyedited and formatted. The final version may differ from this version.



**Intracellular $[Zn^{2+}]_{free}$ Imaging**

TOV112D or HEK293 cells (40,000 cells/well) were plated on either 8-well BD Falcon chambered culture slides (Corning Life Sciences) or 8-chambered #1.5 Nunc Lab-Tek II chambered coverglasses (Thermo Scientific) treated with poly-L-lysine. After 48 h, cells were washed 2 x 5 min in serum-free media and incubated with 1 μM FZ3-AM for 40 min at 37 ˚C. Cells were then washed 2 x 5 min in either EBSS/H (-)Ca/Mg or phenol-red free DMEM + 10% FBS containing the indicated treatments and incubated for 20 min before imaging. For nuclear colocalization, 1 μg/mL Hoechst 33342 was also included. Cells were imaged using a Zeiss LSM510 META NLO confocal microscope equipped with 37 ˚C environmental control chamber. FZ3 and Hoechst 33342 were excited at 488 nm (argon laser) and 790 nm (Chameleon Ti:sapphire laser), respectively. To determine the kinetics of fluorescence change, each background-subtracted image in the time-lapse series was integrated in ImageJ and normalized to the integrated fluorescence of the first frame after treatment. For quantification of intracellular $[Zn^{2+}]_{free}$, each cell was analyzed in the treated, 50 μM PYR/$ZnCl_2$ (1:1), and 100 μM TPEN images by taking the mean fluorescence of an ROI inside the cell subtracted by an ROI immediately outside the cell measured in ImageJ. The $[Zn^{2+}]_{free}$ for each cell was then calculated by Eqn. 2 (Grynkiewicz *et al.*, 1985; Haase *et al.*, 2006):

Eqn. 2:
$$[Zn^{2+}]_{free} = \frac{F - F_{\min}}{F_{\max} - F} \cdot K_d$$

Where F, $F_{max}$, and $F_{min}$ are fluorescence in the treatment, PYR/$ZnCl_2$, and TPEN images, respectively, and $K_d$ is that of FZ3 for $Zn^{2+}$ (15 nM) (Gee *et al.*, 2002). To minimize the effects of outliers the lowest and highest 5% of cells in each series were rejected, and the remaining values averaged. The number of cells analyzed in each trial ranged from 54-163. For nuclear colocalization, treated, PYR/$ZnCl_2$, and TPEN treated images costained with Hoechst 33342

Downloaded from molpharm.aspetjournals.org at ASPET Journals on April 17, 2024

Molecular Pharmacology Fast Forward. Published on February 20, 2015 as DOI: 10.1124/mol.114.097550
This article has not been copyedited and formatted. The final version may differ from this version.



were aligned and each pixel subjected to Eqn. 2 in MATLAB (MathWorks). The resultant images were Gaussian mean filtered and false-colored by calculated $[Zn^{2+}]_{free}$.

**p53-R175H Immunofluorescence**

DMEM + 10% FBS was treated with 5 g Chelex 100 resin per 100 mL media for 1 h with gentle shaking. The media was then decanted and filtered through a 0.2 µm sterile filter. TOV112D cells were then incubated with 1 µM ZMC1 in untreated media, Chelex-treated media, or media + 10 µM TPEN at 37 ˚C for 2 h, fixed, and stained with PAB240 and PAB1640 as previously described (Yu *et al.*, 2012).

Downloaded from molpharm.aspetjournals.org at ASPET Journals on April 17, 2024

Molecular Pharmacology Fast Forward. Published on February 20, 2015 as DOI: 10.1124/mol.114.097550
This article has not been copyedited and formatted. The final version may differ from this version.



## RESULTS

### ZMC1 is a $Zn^{2+}$ ionophore

We evaluated the ability of ZMC1, NTA ($Zn^{2+}$-binding homolog), and A6 (structural homolog) to increase intracellular $[Zn^{2+}]_{free}$ by treating cells with the fluorescent $Zn^{2+}$ indicator FluoZin-3-AM (FZ3-AM) in complete media and imaging them using confocal microscopy (Fig. 1B) (Gibon *et al.*, 2011). In both HEK293 (non-cancer, p53-WT) and TOV112D (ovarian cancer, p53-R175H) cells, ZMC1 increased intracellular $[Zn^{2+}]_{free}$ as indicated by increased fluorescence, but NTA and A6 did not. This result is consistent with the MC model for ZMC1 function and explains the inability of NTA and A6 to rescue p53-R175H at micromolar concentrations.

To provide physical insight into the mechanism by which ZMC1 increases intracellular $[Zn^{2+}]_{free}$, we solved the x-ray crystal structure of the $[Zn(ZMC1)_2]$ complex (Fig. 2). Consistent with previous results, the stoichiometry is 2:1 (Yu *et al.*, 2014). The thiocarbonyl sulfur anion, thiocarbonyl β-nitrogen, and pyridinyl nitrogen from two deprotonated ZMC1 molecules encapsulate the $Zn^{2+}$ and generate a neutral complex. The chemical preparation of this zinc-ZMC1 complex involved treatment of a mixture of 1.0 equivalent of ZMC1 and 0.5 equivalents of $ZnCl_2$ in heated ethanol with excess triethylamine, thus enolizing the thiosemicarbazone to generate thiolate and form the neutral $[Zn(ZMC1)_2]$ complex. This structure bears some similarity to known ionophores (e.g. valinomycin & crown ethers) with the zinc cradled in a hydrophilic pocket inside a hydrophobic shell (Fig. 3A). We therefore tested if ZMC1 is an ionophore by encapsulating the fluorescent $Zn^{2+}$ indicator RhodZin-3 (RZ-3) inside 1,2-dioleoyl-sn-glycero-3-phosphocholine (DOPC) liposomes and assaying the ability of our compounds to transport $Zn^{2+}$ in and out by monitoring fluorescence (Fig. 3B-D, Table 1). We note that

Downloaded from molpharm.aspetjournals.org at ASPET Journals on April 17, 2024

Molecular Pharmacology Fast Forward. Published on February 20, 2015 as DOI: 10.1124/mol.114.097550
This article has not been copyedited and formatted. The final version may differ from this version.



liposomes co-purified with 4.3 μM internal $Zn^{2+}$, allowing for determination of both import and export rates. $Zn^{2+}$ alone was unable to permeate the liposomal membrane as indicated by the lack of RZ-3 fluorescence increase (Fig. 3C). Addition of ZMC1 caused a dose-dependent increase in the rate of RZ-3 fluorescence increase, indicating that ZMC1 can facilitate the transport of $Zn^{2+}$ into the liposomes, consistent with our ionophore hypothesis.

Of the two control compounds, A6 shuttled $Zn^{2+}$ into the liposomes, but NTA did not. Together with Fig. 1B these results illustrate the requirements of an effective synthetic MC. NTA binds $Zn^{2+}$ with an affinity similar to that of ZMC1, but it cannot cross either liposomal or cellular membranes, likely because it possesses negative charges. A6, on the other hand, lacks charges and is similar in structure to ZMC1, but binds $Zn^{2+}$ weakly ($K_{d,A6}$ = 1.1 μM). It can function as an ionophore in conditions of the liposome experiments where external $[Zn^{2+}]_{free}$ was 10 μM. However, in complete media containing 10% fetal bovine serum (FBS), $Zn^{2+}$-binding proteins from the serum (e.g. albumin) necessarily compete for $Zn^{2+}$ with any putative MC, making the effective $[Zn^{2+}]_{free}$ much lower than $[Zn^{2+}]_{total}$ (see Discussion) (Moran *et al.*, 2012). A6 therefore likely does not increase intracellular $[Zn^{2+}]_{free}$ in culture because $K_{d,A6}$ is greater than extracellular $[Zn^{2+}]_{free}$. Thus, both an appropriate $Zn^{2+}$ $K_d$ and ionophore activity are necessary for ZMC1 activity.

We hypothesized that ZMC1 should be able to traverse lipid bilayers as a free compound, and that this property might be important for its biological activity. For example, if it could only cross membranes as the zinc-bound species then the accumulation of free ZMC1 in cells would limit the increase in intracellular $[Zn^{2+}]_{free}$. To test this, we reversed the $[Zn^{2+}]_{free}$ gradient by adding a large excess of metal ion chelator EDTA to the solution outside of the liposomes and monitored fluorescence in the presence and absence of ZMC1 (Fig. 3D). EDTA alone did not

Downloaded from molpharm.aspetjournals.org at ASPET Journals on April 17, 2024

Molecular Pharmacology Fast Forward. Published on February 20, 2015 as DOI: 10.1124/mol.114.097550
This article has not been copyedited and formatted. The final version may differ from this version.



cause a significant decrease in RZ-3 fluorescence as the liposomal membranes are impermeable to EDTA. After subsequent addition of ZMC1, there was a time dependent decrease in RZ-3 fluorescence. This result indicates that free ZMC1 crossed the liposomal membranes, bound internal $Zn^{2+}$, and transported it back outside the liposome where the metal was then bound by the much stronger chelator EDTA. Thus, ZMC1 can cross DOPC bilayers both as free drug and as the $[Zn(ZMC1)_2]$ complex. Mechanistically, $Zn^{2+}$ is complexed by two deprotonated ZMC1 molecules and transported across membranes as an uncharged species. After crossing, the ZMC1 molecules are "re-protonated" to regenerate neutral ZMC1 and release the bound $Zn^{2+}$ (Fig. 3A).

To ensure that our fluorescence results were due to $Zn^{2+}$ transport and not to non-specific disruption of liposomal membranes, we performed a liposomal leakage assay using the self-quenching fluorophore calcein (Fig. 3E) (Hee Dong, 2005). When calcein is encapsulated at concentrations above 4 mM its fluorescence is decreased via self quenching (Hamann *et al.*, 2002). Leakage is detected by a fluorescence increase as the dye dilutes and its fluorescence dequenches. At the highest concentrations of ZMC1 and $ZnCl_2$ used we did not detect a significant fluorescence increase. Disruption of liposomes can also be detected by alteration of their size distribution. The size distribution of liposomes treated with the highest concentrations of $ZnCl_2$ and ZMC1 was identical to that of untreated liposomes (Supplemental Figure 1). Together, these data indicate the liposomal membranes remained intact upon ZMC1 treatment, and therefore the RZ-3 fluorescence changes are attributable only to specific $Zn^{2+}$ transport.

**Characterization of ZMC1-mediated $Zn^{2+}$ transport in live cells**

To extend our investigation of ZMC1 as an ionophore to living systems, we quantified ZMC1-mediated $Zn^{2+}$ transport in cells. We first measured the kinetics of intracellular $[Zn^{2+}]_{free}$

Downloaded from molpharm.aspetjournals.org at ASPET Journals on April 17, 2024

Molecular Pharmacology Fast Forward. Published on February 20, 2015 as DOI: 10.1124/mol.114.097550
This article has not been copyedited and formatted. The final version may differ from this version.



increase by loading HEK293 and TOV112D cells with FZ3-AM, treating the cells with ZMC1 and $ZnCl_2$, and monitoring fluorescence by time-lapse microscopy (Fig. 4A, Supplemental Movies 1-10). To minimize the potential for $Zn^{2+}$ contamination and contributions from poorly defined elements in complete media (e.g. FBS), cells were treated and imaged in $Ca^{2+}$ and $Mg^{2+}$-free Earle's Balanced Salt Solution supplemented with 10 mM HEPES pH 7.4 (EBSS/H (-)Ca/Mg). Excess $ZnCl_2$ with the $Zn^{2+}$ ionophore pyrithione (PYR) was used as a positive control (Haase *et al.*, 2006). Excess membrane-permeable $Zn^{2+}$ chelator N,N,N',N'-tetrakis(2-pyridylmethyl)ethane-1,2-diamine (TPEN) was used as a negative control (Bozym *et al.*, 2006). When treated with $ZnCl_2$ alone or ZMC1 alone, neither cell type showed an increase in intracellular $[Zn^{2+}]_{free}$. When treated with both ZMC1 and $ZnCl_2$, both cell lines showed a time dependent increase at two different $ZnCl_2$ concentrations, demonstrating that both ZMC1 and extracellular $Zn^{2+}$ are required. When the fluorescence increases were fit to first-order exponentials, both concentrations of $ZnCl_2$ yielded identical half-lives in their respective cell types, which we combine to report $t_{1/2}$ (HEK293) = 124 ± 20 s and $t_{1/2}$ (TOV112D) = 156 ± 50 s (mean ± SD, n=4).

We then quantified the steady-state intracellular $[Zn^{2+}]_{free}$ of both cell types after treatment with the 2:1 ratio of ZMC1:$ZnCl_2$ judged to be optimal in our previous manuscript (Fig. 4B-E) (Yu *et al.*, 2014). Cells were again loaded with FZ3-AM, treated with 1 μM ZMC1 and 0.5 μM $ZnCl_2$ in EBSS/H (-)Ca/Mg, and imaged as above. To normalize for differential dye loading, cells were then sequentially treated with excess PYR/$ZnCl_2$, imaged, treated with TPEN, and imaged again. PYR/$ZnCl_2$ and TPEN served to saturate and apoize the intracellular FZ3, respectively (18,20). In the absence of drug we measured intracellular $[Zn^{2+}]_{free}$ of 0.69 ± 0.25 nM for HEK293 cells and 0.71 ± 0.19 nM for TOV112D cells. These values reflect the lower



Downloaded from molpharm.aspetjournals.org at ASPET Journals on April 17, 2024

Molecular Pharmacology Fast Forward. Published on February 20, 2015 as DOI: 10.1124/mol.114.097550
This article has not been copyedited and formatted. The final version may differ from this version.



limit of detection by FZ3-AM and are likely overestimates. Upon treatment with ZMC1 and $ZnCl_2$, intracellular $[Zn^{2+}]_{free}$ rose to 18.1 ± 4.7 nM for HEK293 cells and 15.8 ± 2.5 nM for TOV112D cells. These concentrations are theoretically sufficient to reactivate ~90 % of p53-R175H based on the $K_{d1}$ value of 2.1 nM measured for DBD-R175H (Yu *et al.*, 2014).

**Extracellular $Zn^{2+}$ is necessary for ZMC1 function in cells**

If ZMC1 is a $Zn^{2+}$ ionophore and the source of the $Zn^{2+}$ it delivers is extracellular as suggested by our kinetic experiments in $Zn^{2+}$-free media, then depleting the extracellular $Zn^{2+}$ from complete media should inhibit ZMC1's function. To test this prediction we took advantage of ZMC1's known ability to induce a conformational change in p53-R175H using the conformation specific antibodies PAB240 and PAB1620 in complete media with and without $Zn^{2+}$ chelators (Fig. 5A) (Yu *et al.*, 2012). Consistent with previous results, ZMC1 treatment shifted the p53-R175H immunophenotype from misfolded (PAB240) to WT-like (PAB1620) in TOV112D cells in untreated media (Yu *et al.*, 2012). This shift disappeared when the media was pretreated with metal-ion chelating resin Chelex. Antibody shift was also reduced when the media was treated with the $Zn^{2+}$-selective chelator TPEN. These data confirm the requirement for an extracellular source of ions for ZMC1 function, and that the likely identity of that ion is $Zn^{2+}$.

Because the majority of mutant p53 staining occurs in the nucleus (Fig. 5A), we hypothesized that ZMC1 increases $[Zn^{2+}]_{free}$ in the nucleus as well as the cytosol. As a test we loaded HEK293 and TOV112D cells with FZ3-AM, treated with 2:1 ZMC1/$ZnCl_2$ in EBSS/H (-)Ca/Mg for 20 min, and co-stained the nuclei with Hoechst 33342. To account for differential dye loading in the cytosol, nucleus, endosomes, and other sub-cellular compartments, we

Downloaded from molpharm.aspetjournals.org at ASPET Journals on April 17, 2024

Molecular Pharmacology Fast Forward. Published on February 20, 2015 as DOI: 10.1124/mol.114.097550
This article has not been copyedited and formatted. The final version may differ from this version.



sequentially imaged the cells after ZMC1/$ZnCl_2$, PYR/$ZnCl_2$, and TPEN treatment, calculated the $[Zn^{2+}]_{free}$ profiles, and overlaid the outlines of the nuclei (Fig. 5B-C). $[Zn^{2+}]_{free}$ was relatively homogenous throughout the cells in both cell types; no significant differences between the cytosol and nuclei were observed.

Because thiosemicarbazones like ZMC1 are known to interact with a number of metals involved in a variety of biological processes (e.g. $Fe^{2+}$, $Zn^{2+}$, $Cu^{2+}$, $Mn^{2+}$, $Co^{2+}$, $Ca^{2+}$, and $Mg^{2+}$) we wanted to evaluate ZMC1's potential to interact with other biologically relevant ions (Yu *et al.*, 2009). To this end, we measured absorbance spectra of ZMC1 in the presence of the two most biologically prevalent group II metals ($Ca^{2+}$ and $Mg^{2+}$) and the three most biologically prevalent transition metals ($Fe^{2+/3+}$, $Zn^{2+}$, and $Cu^{2+}$) (Supplemental Figure 2). Neither of the group II metals caused a shift in absorbance. By contrast, all three transition metals produced a shift, indicating that ZMC1 interacts with $Cu^{2+}$, $Fe^{2+}$, and $Fe^{3+}$ in addition to $Zn^{2+}$. This finding is significant for two reasons. First, we previously observed that apoptosis induced by ZMC1 was dependent upon reactive oxygen species generation, which we hypothesized was a result of Fenton chemistry facilitated by ZMC1 interacting with redox-active metals (Yu *et al.*, 2014). Both iron and copper are redox-active, supporting that hypothesis. Second, the lack of an interaction between ZMC1 and $Ca^{2+}$ and $Mg^{2+}$ indicates that $Ca^{2+}$ and $Mg^{2+}$ homeostasis and signaling are unlikely to be perturbed by ZMC1.

Downloaded from molpharm.aspetjournals.org at ASPET Journals on April 17, 2024

Molecular Pharmacology Fast Forward. Published on February 20, 2015 as DOI: 10.1124/mol.114.097550
This article has not been copyedited and formatted. The final version may differ from this version.



**DISCUSSION**

In this study we demonstrate that ZMC1 increases intracellular $[Zn^{2+}]_{free}$ by shuttling extracellular $Zn^{2+}$ ions across the plasma membrane, thus providing a physical mechanism linking ZMC1's ability to buffer $[Zn^{2+}]$ *in vitro* and its ability to reactivate p53-R175H (and other $Zn^{2+}$-binding mutants) *in vivo* (Yu *et al.*, 2012, 2014). We can now define two properties that are necessary and sufficient for a synthetic MC to rescue p53-R175H in cells. The first is that the compound must bind $Zn^{2+}$ with an affinity greater than that of the non-native site(s) on p53 ($K_{d2}$ > $10^{-6}$ M) and that of albumin in serum ($K_{d,albumin}$ ~$10^{-7}$ M; see below), but with an affinity less than that of the native zinc-binding site on p53-R175H ($K_{d1}$ = 2.1 nM) (Masuoka *et al.*, 1993; Yu *et al.*, 2014). The second property is that the compound must be able to transport $Zn^{2+}$ across the plasma membrane.

The above requirements explain why NTA and A6 fail as synthetic MC drugs. NTA and ZMC1 bind $Zn^{2+}$ with comparable affinities and they both reactivate apoDBD-R175H *in vitro*, but NTA does not elevate intracellular $[Zn^{2+}]_{free}$ in cells, at least when dosed at micromolar concentrations (Fig. 1B) (Yu *et al.*, 2014). Like EDTA, NTA possesses multiple negative charges which render it impermeable to cells. By contrast, A6 fails to restore function to apoDBD-R175H *in vitro* because it binds $Zn^{2+}$ too weakly to protect against metal-induced misfolding (Yu *et al.*, 2014). A6 fails to reactivate p53-R175H in cells for a related but different reason. The uncharged A6 molecule can deliver $Zn^{2+}$ across biological membranes, but, owing to its poor $Zn^{2+}$ affinity ($K_{d,A6}$ = 1.1 µM), does so only at high $[Zn^{2+}]_{free}$ (e.g. 10 µM in Fig. 2). *In vivo,* serum $[Zn^{2+}]_{total}$ is typically 8.5-23.6 µM, but nearly all is bound to albumin. The combination of ~0.6 mM albumin and $K_{d,albumin}$ ~$10^{-7}$ M ensures that $[Zn^{2+}]_{free}$ is significantly lower than $K_{d,A6}$ (Masuoka *et al.*, 1993; Ohyoshi *et al.*, 1999; Moran *et al.*, 2012). $[Zn^{2+}]_{free}$ in



Downloaded from molpharm.aspetjournals.org at ASPET Journals on April 17, 2024

Molecular Pharmacology Fast Forward. Published on February 20, 2015 as DOI: 10.1124/mol.114.097550
This article has not been copyedited and formatted. The final version may differ from this version.



culture media is similarly low because the vast majority of $Zn^{2+}$ comes from supplemented serum and is also mostly bound to albumin (Sigma-Aldrich, 2014). Because A6 cannot compete with albumin for $Zn^{2+}$ ($K_{d,A6}$ is 10-fold higher than $K_{d,albumin}$), it follows that A6 cannot bind $Zn^{2+}$ in serum or complete media. Thus, we estimate that an effective MC drug should have a $Zn^{2+}$ $K_d$ in the range $10^{-9}$ to $10^{-7}$ M, defined at either end by $K_{d1}$ of p53-R175H and $K_{d,albumin}$, respectively.

While ZMC1 functions primarily through its interaction with $Zn^{2+}$, we show that it can also interact with redox-active transition metals $Cu^{2+}$ and $Fe^{2+/3+}$. As previously demonstrated, interactions with one or both metals is likely required for ZMC1-induced apoptosis via ROS generation (Yu *et al.*, 2014). However, nearly all iron and copper in serum is bound in high-affinity complexes with transferrin ($K_d < 10^{-19}$ M) for $Fe^{2+/3+}$ and either ceruloplasmin (95%) or albumin ($K_d < 10^{-11}$ M) for $Cu^{2+}$ (Neumann and Sass-Kortsak, 1967; Aisen *et al.*, 1978; Masuoka *et al.*, 1993). Because the resulting concentrations of free iron and copper in serum are expected to be extremely low, and because ZMC1 cannot compete with transferrin and cerulopasmin for metal binding, it is unlikely that ZMC1 will perturb iron or copper homeostasis by transporting these metals into cells. This view is substantiated by the prior observation that ZMC1 is relatively non-toxic to cells and mice lacking mutant p53 (Yu *et al.*, 2014).

It is important to note that the pharmacophore of the ZMC1-Zn complex is the $Zn^{2+}$ ion, with ZMC1 serving exclusively as a metal transport and buffering system. This unusual relationship presents a number of considerations not encountered in traditional pharmacotherapy. A major advantage of synthetic MCs is that they obviate the major hurdle associated with developing conventional targeted chemotherapy drugs: the need to identify compounds that bind to target proteins with high affinity and specificity. Since synthetic MCs need not interact directly with their clients, their structures can vary drastically provided that they maintain their

Downloaded from molpharm.aspetjournals.org at ASPET Journals on April 17, 2024

Molecular Pharmacology Fast Forward. Published on February 20, 2015 as DOI: 10.1124/mol.114.097550
This article has not been copyedited and formatted. The final version may differ from this version.



ability to bind and transport $Zn^{2+}$ into the cell. Indeed, the D'Orazi group recently demonstrated the ability of a bipyridine-$Zn^{2+}$-curcumin complex to reactivate mutant p53-R175H as well as cross the blood-brain barrier (Garufi *et al.*, 2013). Although the structure is unrelated to ZMC1, it is possible that it functions via a similar mechanism. MCs may allow a level of design freedom not possible with conventional drugs, as structures can be varied to optimize pharmacological characteristics (delivery, toxicity, clearance, etc.) without regard to maintaining affinity for p53. A second consideration is that, because MC-mediated p53 restoration is caused by increasing intracellular $[Zn^{2+}]_{free}$ to an optimum level, co-administration of zinc supplements or pre-forming the $Zn^{2+}$ complex may increase the effectiveness of MCs if the $[Zn^{2+}]$ in the serum is insufficient to reach this target. Therefore, defining the optimal serum $[Zn^{2+}]$ and the most efficient method to maintain that level may enhance the therapeutic potential of MCs.

Downloaded from molpharm.aspetjournals.org at ASPET Journals on April 17, 2024

Molecular Pharmacology Fast Forward. Published on February 20, 2015 as DOI: 10.1124/mol.114.097550
This article has not been copyedited and formatted. The final version may differ from this version.



## AUTHOR CONTRIBUTIONS

Participated in research design: Blanden, Yu, Wolfe, Augeri, O'Dell, Olson, Kimball, Movileanu, Carpizo, and Loh.

Conducted experiments: Blanden, Yu, Wolfe, Gilleran, Augeri, and Emge.

Contributed new reagents or analytic tools: Gilleran, Augeri, and Emge.

Performed Data Analysis: Blanden, Yu, Gilleran, Augeri, Kimball, Emge, and Loh.

Wrote or contributed to the writing of the manuscript: Blanden, Yu, Augeri, and Loh.

Downloaded from molpharm.aspetjournals.org at ASPET Journals on April 17, 2024

Molecular Pharmacology Fast Forward. Published on February 20, 2015 as DOI: 10.1124/mol.114.097550
This article has not been copyedited and formatted. The final version may differ from this version.



**REFERENCES**

Aisen P, Leibman A, and Zweier J (1978) Stoichiometric and site characteristics of the binding of iron to human transferrin. *J Biol Chem* 253:1930–1937.

Bozym RA, Thompson RB, Stoddard AK, and Fierke CA (2006) Measuring Picomolar Intracellular Exchangeable Zinc in PC-12 Cells Using a Ratiometric Fluorescence Biosensor. *ACS Chem Biol* 1:103–111.

Bullock AN, Henckel J, DeDecker BS, Johnson CM, Nikolova PV, Proctor MR, Lane DP, and Fersht AR (1997) Thermodynamic stability of wild-type and mutant p53 core domain. *Proc Natl Acad Sci* 94:14338–14342.

Bullock AN, Henckel J, and Fersht AR (2000) Quantitative analysis of residual folding and DNA binding in mutant p53 core domain: definition of mutant states for rescue in cancer therapy. *Oncogene* 19:1245–1256.

Butler JS, and Loh SN (2003) Structure, function, and aggregation of the zinc-free form of the p53 DNA binding domain. *Biochemistry (Mosc)* 42:2396–2403.

Butler JS, and Loh SN (2007) Zn(2+)-dependent misfolding of the p53 DNA binding domain. *Biochemistry (Mosc)* 46:2630–2639.

Cho Y, Gorina S, Jeffrey PD, and Pavletich NP (1994) Crystal structure of a p53 tumor suppressor-DNA complex: understanding tumorigenic mutations. *Science* 265:346–355.

Colvin RA, Holmes WR, Fontaine CP, and Maret W (2010) Cytosolic zinc buffering and muffling: their role in intracellular zinc homeostasis. *Met Integr Biometal Sci* 2:306–317.

Downloaded from molpharm.aspetjournals.org at ASPET Journals on April 17, 2024

Molecular Pharmacology Fast Forward. Published on February 20, 2015 as DOI: 10.1124/mol.114.097550
This article has not been copyedited and formatted. The final version may differ from this version.



Garufi A, Trisciuoglio D, Porru M, Leonetti C, Stoppacciaro A, D'Orazi V, Avantaggiati ML, Crispini A, Pucci D, and D'Orazi G (2013) A fluorescent curcumin-based Zn(II)-complex reactivates mutant (R175H and R273H) p53 in cancer cells. *J Exp Clin Cancer Res* 32:72.

Gee KR, Zhou Z-L, Ton-That D, Sensi SL, and Weiss JH (2002) Measuring zinc in living cells.: A new generation of sensitive and selective fluorescent probes. *Cell Calcium* 31:245–251.

Gibon J, Tu P, Bohic S, Richaud P, Arnaud J, Zhu M, Boulay G, and Bouron A (2011) The over-expression of TRPC6 channels in HEK-293 cells favours the intracellular accumulation of zinc. *Biochim Biophys Acta* 1808:2807–2818.

Grynkiewicz G, Poenie M, and Tsien RY (1985) A new generation of Ca2+ indicators with greatly improved fluorescence properties. *J Biol Chem* 260:3440–3450.

Haase H, Hebel S, Engelhardt G, and Rink L (2006) Flow cytometric measurement of labile zinc in peripheral blood mononuclear cells. *Anal Biochem* 352:222–230.

Hamann S, Kiilgaard JF, Litman T, Alvarez-Leefmans FJ, Winther BR, and Zeuthen T (2002) Measurement of Cell Volume Changes by Fluorescence Self-Quenching. *J Fluoresc* 12:139–145.

Hee Dong TWK (2005) Release of calcein from temperature-sensitive liposomes in a poly (N-isopropylacrylamide) hydrogel. *Macromol Res* 13:54–61.

Downloaded from molpharm.aspetjournals.org at ASPET Journals on April 17, 2024

Molecular Pharmacology Fast Forward. Published on February 20, 2015 as DOI: 10.1124/mol.114.097550
This article has not been copyedited and formatted. The final version may differ from this version.



Levine AJ, and Oren M (2009) The first 30 years of p53: growing ever more complex. *Nat Rev Cancer* 9:749–758.

Loh SN (2010) The missing zinc: p53 misfolding and cancer. *Met Integr Biometal Sci* 2:442–449.

Masuoka J, Hegenauer J, Van Dyke BR, and Saltman P (1993) Intrinsic stoichiometric equilibrium constants for the binding of zinc(II) and copper(II) to the high affinity site of serum albumin. *J Biol Chem* 268:21533–21537.

Méplan C, Richard MJ, and Hainaut P (2000) Metalloregulation of the tumor suppressor protein p53: zinc mediates the renaturation of p53 after exposure to metal chelators in vitro and in intact cells. *Oncogene* 19:5227–5236.

Moran VH, Stammers A-L, Medina MW, Patel S, Dykes F, Souverein OW, Dullemeijer C, Pérez-Rodrigo C, Serra-Majem L, Nissensohn M, and Lowe NM (2012) The relationship between zinc intake and serum/plasma zinc concentration in children: a systematic review and dose-response meta-analysis. *Nutrients* 4:841–858.

Neumann PZ, and Sass-Kortsak A (1967) The state of copper in human serum: evidence for an amino acid-bound fraction. *J Clin Invest* 46:646–658.

Ohyoshi E, Hamada Y, Nakata K, and Kohata S (1999) The interaction between human and bovine serum albumin and zinc studied by a competitive spectrophotometry. *J Inorg Biochem* 75:213–218.

Downloaded from molpharm.aspetjournals.org at ASPET Journals on April 17, 2024

Molecular Pharmacology Fast Forward. Published on February 20, 2015 as DOI: 10.1124/mol.114.097550
This article has not been copyedited and formatted. The final version may differ from this version.



Olivier M, Hollstein M, and Hainaut P (2010) TP53 Mutations in Human Cancers: Origins, Consequences, and Clinical Use. *Cold Spring Harb Perspect Biol* 2.

Sigma-Aldrich (2014) Zinc in Cell Culture - uses of zinc in serum-free eucaryotic, including hybridoma.

Ventura A, Kirsch DG, McLaughlin ME, Tuveson DA, Grimm J, Lintault L, Newman J, Reczek EE, Weissleder R, and Jacks T (2007) Restoration of p53 function leads to tumour regression in vivo. *Nature* 445:661–665.

Xue W, Zender L, Miething C, Dickins RA, Hernando E, Krizhanovsky V, Cordon-Cardo C, and Lowe SW (2007) Senescence and tumour clearance is triggered by p53 restoration in murine liver carcinomas. *Nature* 445:656–660.

Yu X, Blanden AR, Narayanan S, Jayakumar L, Lubin D, Augeri D, Kimball SD, Loh SN, and Carpizo DR (2014) Small molecule restoration of wildtype structure and function of mutant p53 using a novel zinc-metallochaperone based mechanism. *Oncotarget* 5:8879–8892.

Yu X, Vazquez A, Levine AJ, and Carpizo DR (2012) Allele-Specific p53 Mutant Reactivation. *Cancer Cell* 21:614–625.

Yu Y, Kalinowski DS, Kovacevic Z, Siafakas AR, Jansson PJ, Stefani C, Lovejoy DB, Sharpe PC, Bernhardt PV, and Richardson DR (2009) Thiosemicarbazones from the Old to New: Iron Chelators That Are More Than Just Ribonucleotide Reductase Inhibitors. *J Med Chem* 52:5271–5294.

Downloaded from molpharm.aspetjournals.org at ASPET Journals on April 17, 2024

Molecular Pharmacology Fast Forward. Published on February 20, 2015 as DOI: 10.1124/mol.114.097550
This article has not been copyedited and formatted. The final version may differ from this version.



**FOOTNOTES**

This work was supported by grants from the National Institutes of Health National Cancer Institute [K08CA172676-02], the Breast Cancer Research Foundation, the Harrington Discovery Institute, and the Sidney Kimmel Foundation for Cancer Research to DRC, the Carol M. Baldwin Breast Cancer Research Award to SNL, and the National Institutes of Health National Institute of General Medical Sciences [R01GM088403] to LM.

Downloaded from molpharm.aspetjournals.org at ASPET Journals on April 17, 2024

Molecular Pharmacology Fast Forward. Published on February 20, 2015 as DOI: 10.1124/mol.114.097550
This article has not been copyedited and formatted. The final version may differ from this version.



## FIGURE LEGENDS

**Figure 1. ZMC1 treatment in complete media increases intracellular $[Zn^{2+}]_{free}$. A)** Structures of compounds used in this study and their $K_d$s for $Zn^{2+}$. $K_d$s shown from Yu *et al.*, 2014. **B)** Imaging of intracellular $Zn^{2+}$ level in complete media. HEK293 and TOV112D cells were loaded with FZ3-AM followed by 1 µM of the indicated treatment in 0.2% DMSO for 20 min at 37 ˚C and imaged using a 20X (NA=0.75) air objective. Scale bar = 100 µm.

**Figure 2. Molecular Structure of $[Zn(ZMC1)_2]$ by X-ray Crystallography.** C = gray, N = dark blue, S = yellow, Zn = aqua blue. Data are available in Supplemental Tables 1-6. X-ray data show significant single bond character of the C-S bond (1.726 Å) to support enolization of ZMC1.

**Figure 3. ZMC1 is an ionophore in a liposomal model system. A)** Diagram of ZMC1 mediated $Zn^{2+}$ transport. $Zn^{2+}$ combines with two enolizable ZMC1 molecules to generate an overall neutral complex that moves across the membrane. After crossing, the complex dissociates to release two ZMC1 molecules and free $Zn^{2+}$. **B)** Schematic of the liposomal system. Charges omitted for clarity. **C-D)** $Zn^{2+}$ import (C) and export (D) kinetics measured by DOPC-encapsulated RZ-3 fluorescence. RZ-3 was encapsulated at 10 µM. Arrows indicate treatment addition. TritonX-100 and DMSO were positive and vehicle controls, respectively. Concentrations were: 10 µM $ZnCl_2$, 100 µM EDTA, 5 µM NTA, 5 µM A6, 1% TritonX-100, 0.2% DMSO, and 1 or 5 µM ZMC1. Quantification is shown in Table 1. **E)** Calcein leakage assay. Calcein (10 mM) was DOPC-encapsulated and subjected to the indicated treatments.

Downloaded from molpharm.aspetjournals.org at ASPET Journals on April 17, 2024

Molecular Pharmacology Fast Forward. Published on February 20, 2015 as DOI: 10.1124/mol.114.097550
This article has not been copyedited and formatted. The final version may differ from this version.



Arrows indicate treatment addition. TritonX-100 and DMSO were positive and vehicle controls, respectively. Concentrations as in C-D.

**Figure 4. Quantification of ZMC1-mediated intracellular $[Zn^{2+}]_{free}$ increase. A)** Representative kinetic traces of intracellular $[Zn^{2+}]$ increase in HEK293 and TOV112D cells. Cells were loaded with FZ3-AM and exchanged into EBSS/H (-)Ca/Mg. Cells were then given the indicated treatment and monitored by time-lapse microscopy. Results are shown as total fluorescence relative to the first frame after treatment (shown as t = 0). PYR/$ZnCl_2$ and DMSO were used as positive and loading controls, respectively. TPEN (100 µM) was added at the arrow as a negative control. Representative videos are included as Supplemental Movies 1-10). **B-C)** Representative images of HEK293 (B) or TOV112D (C) cells loaded with FZ3-AM either untreated or treated with 1 µM ZMC1/0.5 µM $ZnCl_2$ in EBSS/H (-)Ca/Mg for 20 min, followed by 50 µM PYR/50 µM $ZnCl_2$ and 100 µM TPEN. Images were taken using a 10X (NA = 0.3) air objective. Scale bar = 100 µm **D-E)** Quantification of images represented in (B) and (C) respectively according to Eqn. 2. Results are mean ± SD (n = 3). *p<0.003, **p<0.0005

**Figure 5. Extracellular $Zn^{2+}$ is required for ZMC1-induced p53 conformation change. A)** Immunophenotype analysis of R175H-p53 in TOV112D cells. Cells were treated with 1 µM ZMC1 in complete media, Chelex-treated media, and TPEN-treated media for 2 h, fixed, and assayed via immunofluorescence microscopy with the indicated primary antibodies. Scale bars = 100 µm. **B)** ZMC1/$ZnCl_2$ treated HE293 (left) and TOV112D (right) cells false-colored by $[Zn^{2+}]_{free}$. Cells were loaded with FZ3-AM and treated with 1 µM ZMC1/0.5 µM $ZnCl_2$ in EBSS/H (-)Ca/Mg for 20 min. $[Zn^{2+}]_{free}$ was calculated from images of the treatment, 50 µM

Downloaded from molpharm.aspetjournals.org at ASPET Journals on April 17, 2024

Molecular Pharmacology Fast Forward. Published on February 20, 2015 as DOI: 10.1124/mol.114.097550
This article has not been copyedited and formatted. The final version may differ from this version.



PYR/50 µM $ZnCl_2$, and 100 µM TPEN according to Eqn. 2. Outlines of nuclei from Hoechst 33342 co-staining shown in dark red. Images were taken using a 40X (NA = 1.3) oil immersion objective. Scale bar = 10 µm. **C)** $[Zn^{2+}]_{free}$ profiles indicated by the white dotted line in corresponding images in (B).

Downloaded from molpharm.aspetjournals.org at ASPET Journals on April 17, 2024

Molecular Pharmacology Fast Forward. Published on February 20, 2015 as DOI: 10.1124/mol.114.097550
This article has not been copyedited and formatted. The final version may differ from this version.



**TABLES**

**Table 1. Initial $Zn^{2+}$ Ion Flux into DOPC Liposomes.** Fluxes were calculated from linear fits of initial fluorescence changes in the time-courses represented in Fig. 2 using Eqn. 1. Values are mean ± SD (n ≥3).

| Sample | $J_i$ (mol $m^{-2}$ $s^{-1}$) ($10^{-14}$) |
|---|---|
| $ZnCl_2$ Only (10 μM) | 8.90 ± 0.94 |
| $ZnCl_2$ + DMSO (0.2%) | 6.81 ± 0.68 |
| $ZnCl_2$ + ZMC1 (1 μM) | 52.3 ± 1.2 |
| $ZnCl_2$ + ZMC1 (5 μM) | 135 ± 5 |
| $ZnCl_2$ + NTA (5 μM) | 4.52 ± 1.22 |
| $ZnCl_2$ + A6 (5 μM) | 71.3 ± 2.9 |
| EDTA Only (100 μM) | -0.69 ± 0.67 |
| EDTA + DMSO (0.2%) | -0.53 ± 1.43 |
| EDTA + ZMC1 (1 μM) | -131 ± 2 |
| EDTA + ZMC1 (5 μM) | -199 ± 86 |

Downloaded from molpharm.aspetjournals.org at ASPET Journals on April 17, 2024

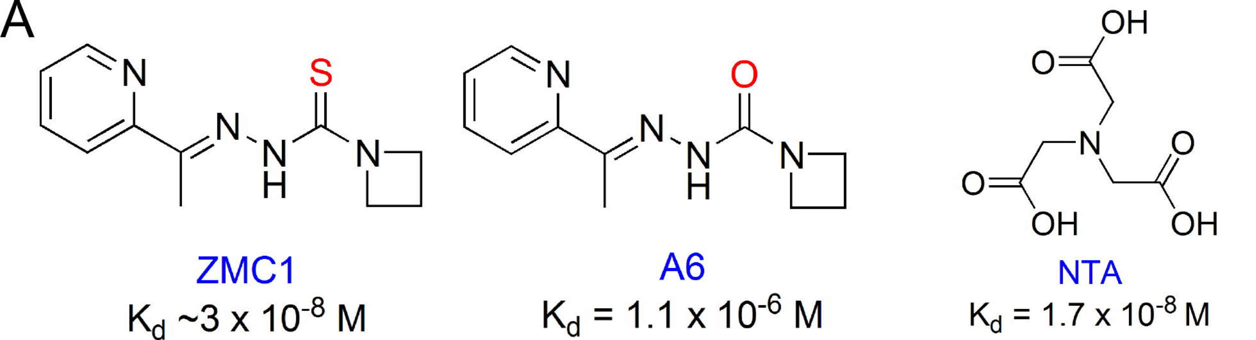


Figure 1

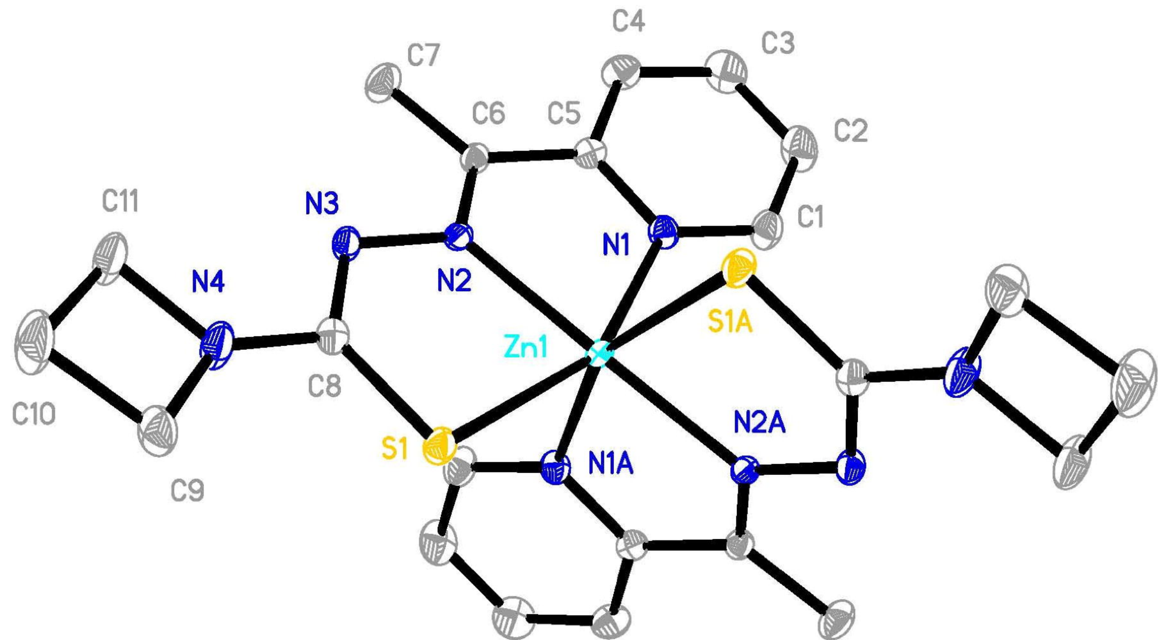


Figure 2

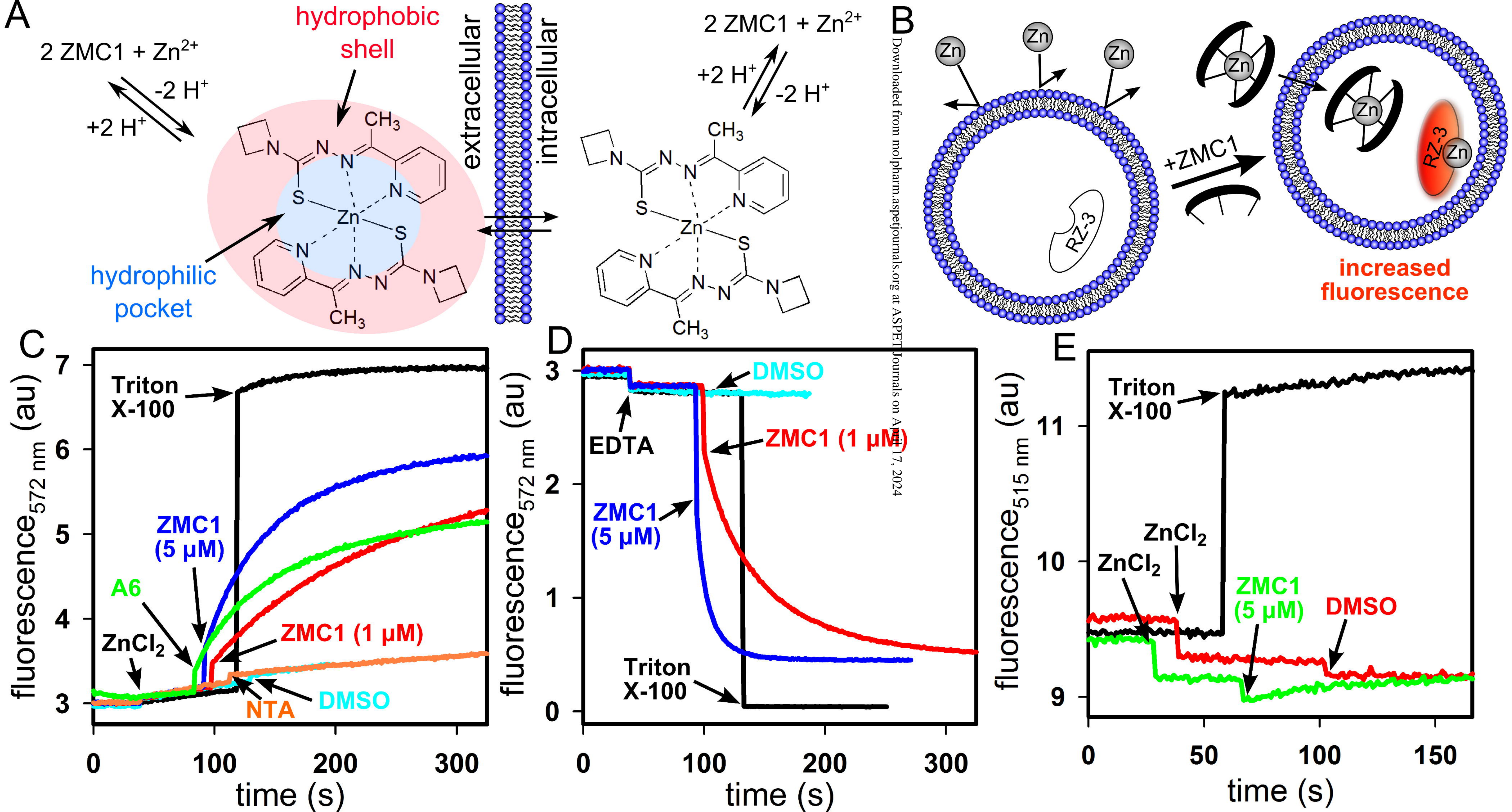

Downloaded from molpharm.aspetjournals.org at ASPET Journals on April 17, 2024

Figure 3

A

HEK293

TOV112D

f/f0

2.5
2.0
1.5
1.0
0.5

TPEN

0 100 200 300 400 500

time (s)

50 μM PYR/$ZnCl_2$ (1:1)

1 μM ZMC1 alone

10 μM $ZnCl_2$+ 0.2% DMSO

1 μM ZMC1 + 10 μM $ZnCl_2$

1 μM ZMC1 + 1 μM $ZnCl_2$

Molecular Pharmacology Fast Forward. Published on February 20, 2015 as DOI: 10.1124/mol.114.097
This article has not been copyedited and formatted. The final version may differ from this version.

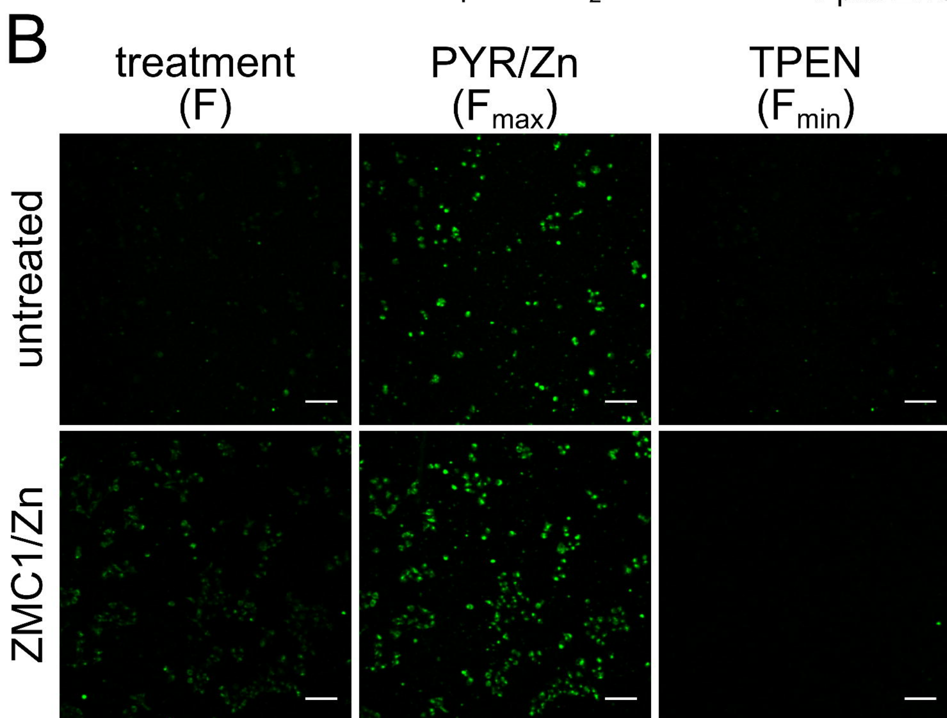


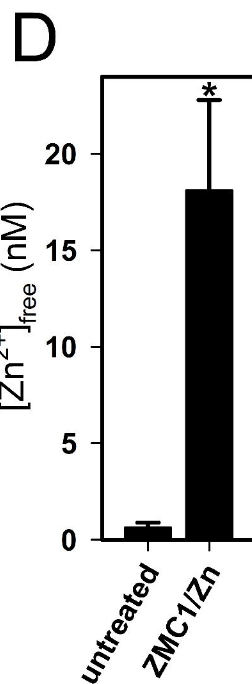


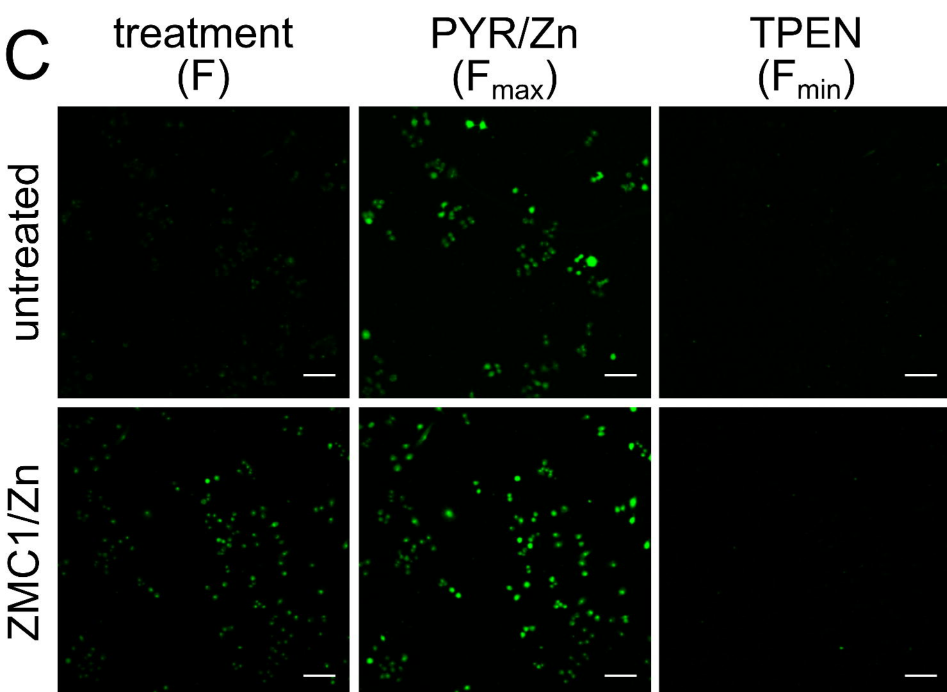


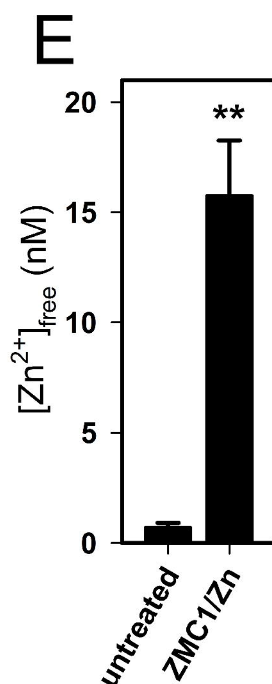


Figure 4

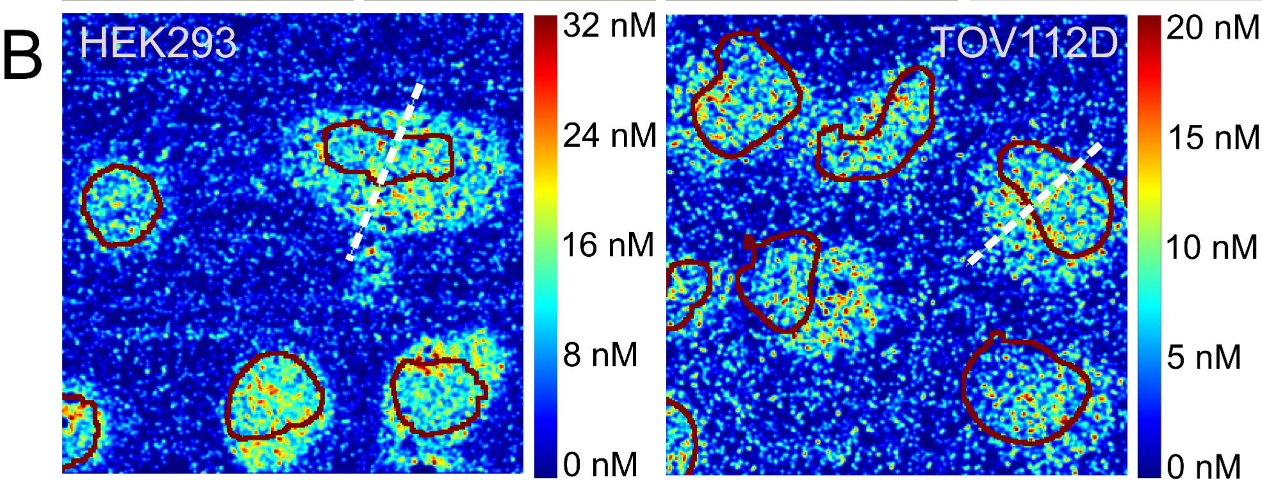


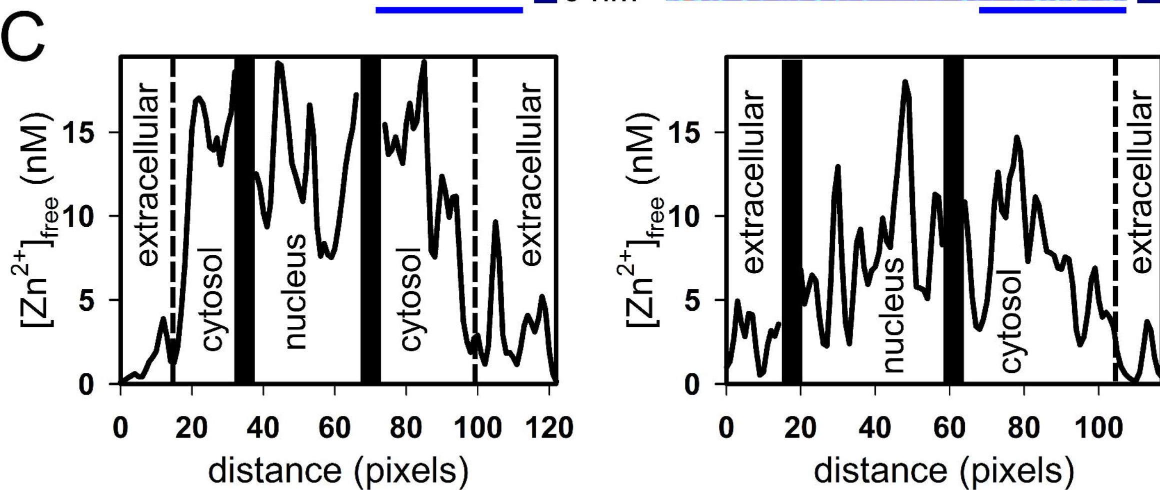


Figure 5